Eur. Phys. J. B **47**, 571–581 (2005)
DOI: 10.1140/epjb/e2005-00354-5

THE EUROPEAN PHYSICAL JOURNAL B

Growth-driven percolations: the dynamics of connectivity in neuronal systems

L. da Fontoura Costa[1,a] and R.C. Coelho[2,b]

[1] Cybernetic Vision Research Group, DFI-IFSC, Universidade de São Paulo, São Carlos, SP, Caixa Postal 369, 13560-970, Brasil
[2] Faculdade de Ciências Matemáticas, da Natureza e Tecnologia de Informação - Methodist University of Piracicaba, Rodovia do Açúcar, km 156 - Campus Taquaral - Taquaral, Piracicaba, SP 13400-901, Brazil

Received 22 December 2004 / Received in final form 9 June 2005
Published online 17 November 2005 –

Abstract. The quintessential property of neuronal systems is their intensive patterns of selective synaptic connections. The current work describes a physics-based approach to neuronal shape modeling and synthesis and its consideration for the simulation of neuronal development and the formation of neuronal communities. Starting from images of real neurons, geometrical measurements are obtained and used to construct probabilistic models which can be subsequently sampled in order to produce morphologically realistic neuronal cells. Such cells are progressively grown while monitoring their connections along time, which are analysed in terms of percolation concepts. However, unlike traditional percolation, the critical point is verified along the growth stages, not the density of cells, which remains constant throughout the neuronal growth dynamics. It is shown, through simulations, that growing beta cells tend to reach percolation sooner than the alpha counterparts with the same diameter. Also, the percolation becomes more abrupt for higher densities of cells, being markedly sharper for the beta cells. In the addition to the importance of the reported concepts and methods to computational neuroscience, the possibility of reaching percolation through morphological growth of a fixed number of objects represents in itself a novel paradigm of great theoretical and practical interest for the areas of statistical physics and critical phenomena.

PACS. 89.75.Fb Structures and organization in complex systems – 02.10.Ox Combinatorics; graph theory – 87.18.La Morphogenesis – 87.18.Sn Neural networks

The brain is a world consisting of a number of unexplored continents and great stretches of unknown territory. *(Santiago Ramon-y-Cajal)*

Neurons can be understood as cells which, along the evolutionary process, have become highly specialized for establishing connections between themselves along a wide range of spatial scales (ranging from microns to meters). In order to minimize metabolism and allow connections to selective targets, neurons acquired their intricated, ramified shapes. Indeed, instead of implementing casual connections with every surrounding cell, a neuron links to specific targets which can be nearby in the same neuronal region or far away in another cortical area originating, in the process, the basic architecture required for proper operation of the central nervous system. Interestingly, the connectivity pattern of a mature neuronal system is determined not only by the genome, which is unable to code all connections[1], but predominantly by the history of neuronal activity under stimuli presentation. Neurons are produced at ventricular zones of the neuroepithelium, in the form of *neuroblasts*, which therefore differentiate and migrate to specific target regions and start to unfold their dendritic and axonal processes [1]. As such structures develop and extend towards specific targets, which occurs under the guidance of trophic factors, they synapse and start forming communities (or clusters) of connected cells, organized in specific ways so as to achieve proper operation. Indeed, the functional properties of such structures are to a large extent related to the underlying connecting patterns, implying that one of the fundamental problems in neuroscience is to understand how neuronal connections are established during the development of the central nervous system [1].

Since connectivity is the main purpose underlying neuronal growth and organization, it is interesting to obtain suitable mathematical structures and relationships capable of representing and modeling the development of neuronal systems at a high level of morphological realism. Previous related works on activity-dependent neuronal development have been reviewed in [2], and a phase

[a] e-mail: luciano@ifsc.usp.br
[b] e-mail: rccoelho@unimep.br

[1] Indeed, even the fate of neuroblasts along the cell differentiation process often does not involve genetical coding [1].

transition approach to neuronal connectivity has been proposed in [3], where the neuronal cells are represented in terms of circles of growing sizes. While graphs/networks, where neurons are assigned to nodes and synapses to edges, provide a natural means to express the neuronal connections, several concepts from statistical mechanics can be used to model and simulate the connection dynamics. By providing an interesting interface between graph theory and statistical mechanics, the recent area of complex networks [4–6] represents a particularly promising perspective to bridge the gap between the morphology and dynamics of neuronal systems. In particular, the concept of percolation [7] stand out as particularly relevant for such investigations. Previous related works include the statistical physics investigation of scaling properties and the degree of separation in cortical networks [8], the small-world characterization of neuronal structures grown in vitro [9], the use of critical percolation point for neuronal shape characterization [10], and the identification of electrically active clusters in neural networks [11]. Related works addressing the relationship between neuronal geometry and function can also be found in the literature (e.g. [12–15]). While such works have considered static neuronal shapes, the development of a framework to model neuromorphically realistic neurons reported in [16] allows investigations of the neuronal connectivity during simulated neuronal development, by monitoring the size and other properties of the existing clusters in terms of time. Such a perspective motivated the extension of the concept of percolation to consider growing structures where the shapes of the objects may vary with time, a possibility proposed and investigated possibly for the first time in the present work.

This article starts by describing how the neuronal cells are represented and statistically modeled in terms of probabilities and follows by presenting the simulation of neuronal growth by using the Monte Carlo approach, as well as the characterization of the obtained structures in terms of the maximum cluster size observed along time, with special interest given to percolation. Such issues are illustrated with respect to a database of 2D neuronal cells including cat retina ganglionar cells of the types alpha (23 samples) and beta (27 samples), of which typical cells are illustrated in Figure 1. Although growth of real neurons is also influenced by trophic fields emanating from putative targets, the simulations in the current work only takes into account the typical geometrical features observed in mature alpha and beta ganglion retinal cells.

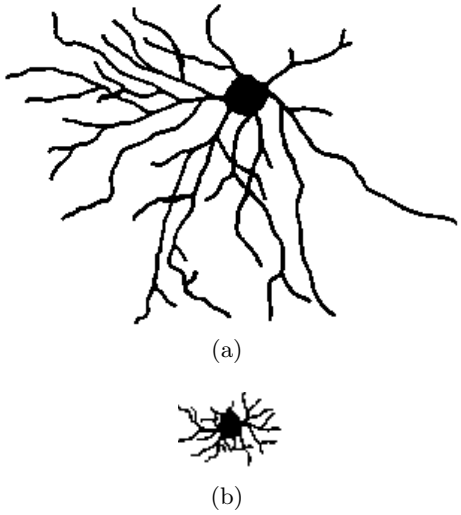

(a)

(b)

Fig. 1. Example of alpha (a), [17], and beta (b) [18] cells used in this work. Reproduced with permission.

1 Neuronal modeling

One first key isse in neuromorphic modeling regards how to represent mathematically the geometry of neurons. While the typically observed diversity of shapes for the same class of cells immediately implies the use of statistics, the choice of the best (in the sense of being the most compact) set of morphometric parameters capable of representing the neuronal shape without considerable loss of information remains a challenging issue [15]. The methodology for 2D neuronal representation adopted in this work follows the framework reported in [16], involving a probabilistic model considering the number of branches, the angles between them, the length of the dendritic and axonal segments, branching probability, and the length and angle of arcs of each branch. Therefore, the first step is to obtain such measurements from images of the real neuronal cells to be modeled. Typically, the cells are histologically marked and prepared, mounted on slides, and the respective images acquired through a camera interfaced to a light transmission (or fluorescence) microscope. The neurons in such images are then identified and isolated (e.g. [19]), producing binary representations (i.e. images containing only the neuronal cell – marked as one, and the background – marked as zero). An alternative way to obtain the binary images of the neural cells is through camera-lucida drawings, as is the case for the images in Figure 1. Once such binary images are obtained, their boundaries are extracted by using a customized neural tracer[2], producing results such as those illustrated in Figure 2, which corresponds to the boundaries of the cells in Figure 1.

The dendrites are henceforth understood as trees, so that the respective hierarchical level can be precisely defined while considering the soma as reference. Therefore, the dendritic segments directly connected to the soma, as well as branching points initiating at such segments, are identified as being at hierarchical level 1, and so on. Our simulations are restricted to a maximum of 10 hierarchical levels, as there are very few branchings occurring at higher levels in the real cells. The probability of branch points for each considered type of cell are shown in Figures 3a and b, respectively for alpha and beta cells. The probabil-

[2] This neural tracer, developed by L.A. Consularo during his Ph.D. at the Cybernetic Vision Research group, allows operator-assisted tracing of the neuronal cells, producing results in the Eutectic format.

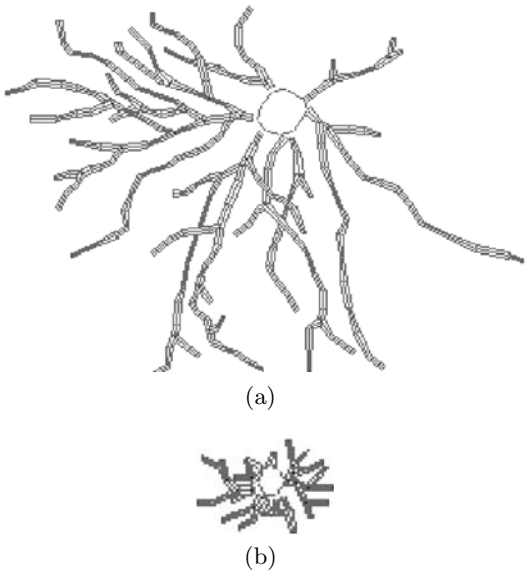

(a)

(b)

Fig. 2. Traced cells obtained from the cells in Figure 1 by using a customized neural tracer.

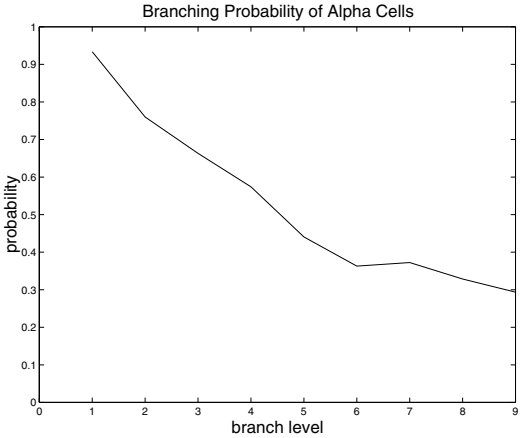

(a)

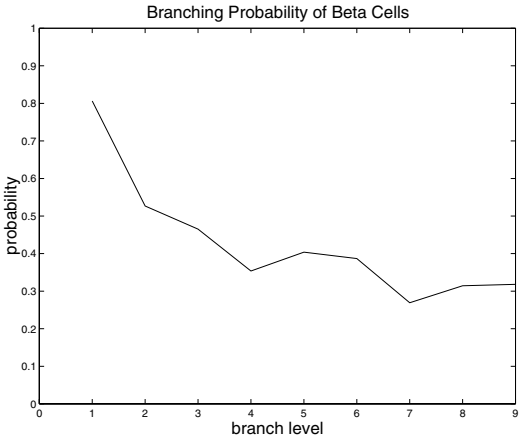

(b)

Fig. 3. Probability function illustrating the branching probability of alpha (a) and beta (b) cells in each level.

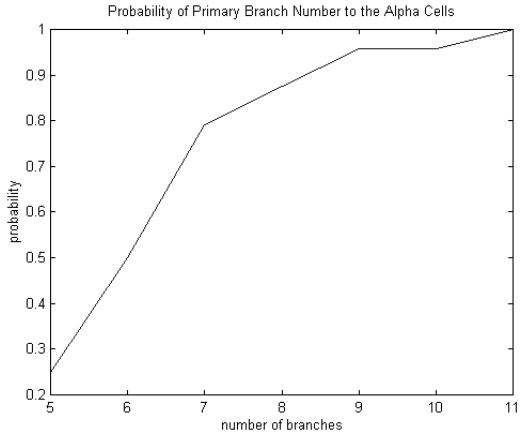

(a)

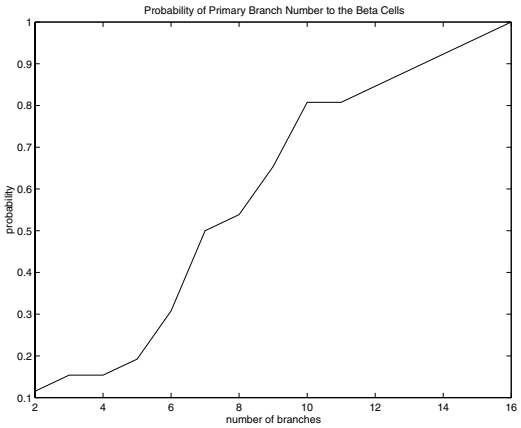

(b)

Fig. 4. Probability function of the number of primary dendritic segments to the alpha (a) and beta (b) cells.

ity of the number of dendritic segments directly attached to the soma (i.e. hierarchical level 1) is also necessary for the statistical model of the growing cells. Figure 4 show the cumulative densities for the alpha (a) and beta (b) neuronal types.

In addition to being essential for neuronal shape modeling, the above branching and initial densities provide interesting information by themselves. For instance, it is clear from the two densities in Figure 3 that the alpha cells are characterized by higher branching rates at the lower hierarchical levels, as is clear from the more accentuated decrease of the respective density along the hierarchical levels. Figure 4 presents the probability of primary branches. The graph in Figure 4(a) shows that the alpha cells present high probability of having from 5 to 7 branches emanating from the soma, while the beta cells have high probability of presenting over 10 branches.

In addition to the above probabilities, it is also necessary to obtain probabilistic models of the dendritic segment arc-lengths. Although alpha cells are typically much larger than beta cells (especially in the periphery of the retina), we used size-normalized versions of the considered neurons in order to have neurons with similar sizes. This

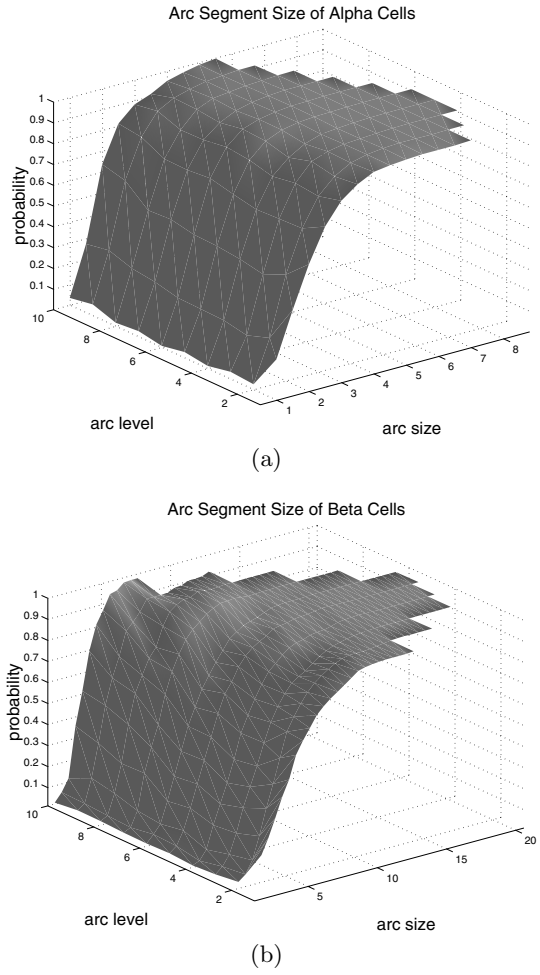

Fig. 5. Distribution function of dendritic segments arc-lengths of the alpha (a) and beta (b) cells.

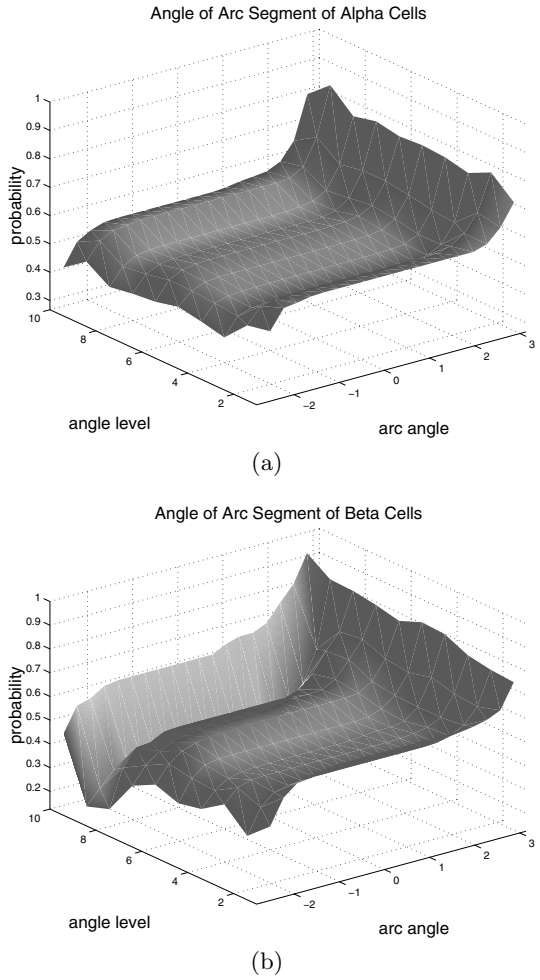

Fig. 6. Distribution function of dendritic segments angles (in radians) of the alpha (a) and beta (b) cells.

allows our percolation study to be mostly defined by the shape intrincacy of the cells rather than their sizes[3]. Figure 5 shows the cumulative two-variated density of such lengths in terms of the hierarchical level for the alpha (a) and beta (b) types of cells, while Figure 6 presents the angles of these dendritic segment arc-lengths for the alpha (a) and beta (b) cells. The last features considered in this work refer to the branch lengths and angles at the branch points, which are shown in Figures 7 and 8 for the alpha (a) and beta (b) cells. By "branch length" it is understood the total arc-length while moving from the branching point to the cell soma, another branch point, or an extremity point.

Note that both branching angle densities (i.e. Figs. 6 and 7) are similar for both alpha and beta cells. The length-related densities (i.e. Figs. 5 and 8) were obtained for alpha cells and then normalized with respect to their respective diameters (i.e. the largest distance between any two points of each cell) in such a way that they have the same average diameter as beta cells. Such a normalization was adopted so that the percolation only reflects the shape (and not size) of the cells.

[3] Given two cells with similar morphologies but different sizes, the larger cell will obviously tend to percolate sooner.

2 Neuronal synthesis

In order to generate the neuronal shapes, the probabilistic model of the neuronal geometry described in the previous section was statistically sampled by the Monte Carlo approach as explained in the following. Initially, the soma of each cell was uniformly (Poisson distribution) distributed along an $N \times N$ matrix (associated to a digital image). The number of branches emerging from the soma was randomly chosen according to the respective density, being uniformly distributed along the somata, which are circular. For each cell, for each branch, the orientation of the emerging segment was drawn from the respective distribution. Straight segments are then incorporated, piece-by-piece, into the growing process. The length and orientation of each of these segment pieces was sampled through Monte Carlo from the respective statistical model. In order to allow all neuronal cells to grow in a "simultaneous" fashion, a single segment piece is incorporated

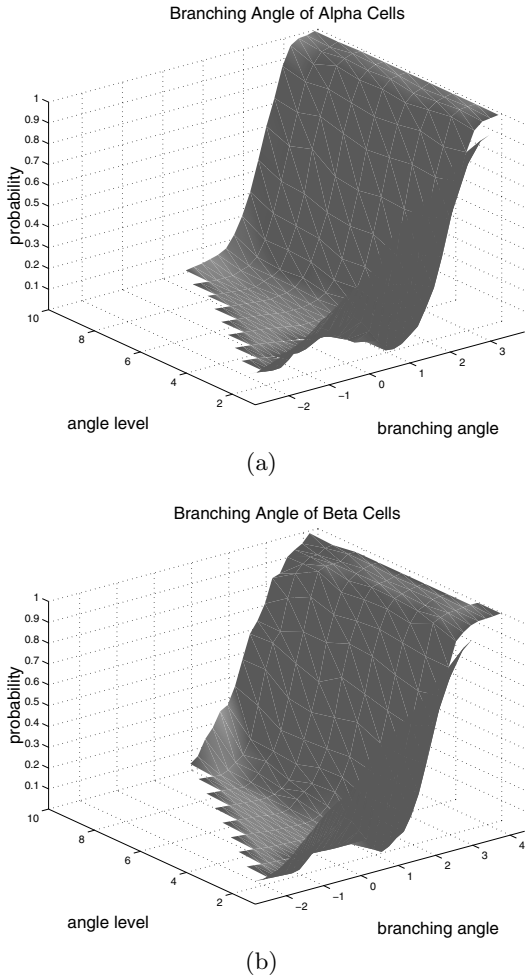

Fig. 7. Distribution function of the angles (in radians) at the branch points of the alpha (a) and beta (b) cells.

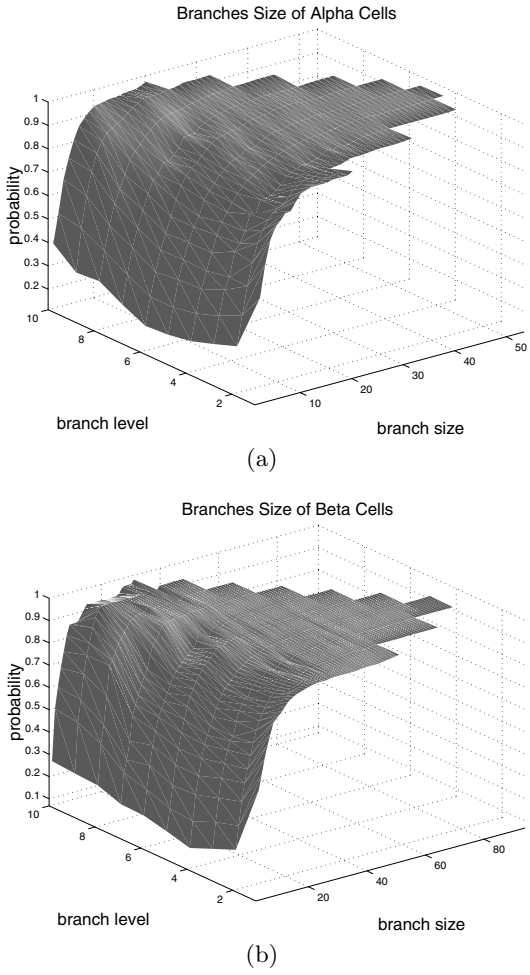

Fig. 8. Distribution function of the branch lengths to the alpha (a) and beta (b) cells.

into each growing branch, for each neuronal cell, at a time ("round-robin" scheme). Every time a new branch was visited, the probability for new branch or growth termination was sampled, and the respective action taken. In case we have a branch[4], the orientations of the two branching new segments were sampled from the respective distributions, and those branches were subsequently included in the "round-robin" growth scheme. The growth of branches continued until one of the following conditions is reached: (a) it is selected for interruption; or (b) it reached 10 hierarchical stages. Figure 9 illustrates morphologically-realistic neuronal networks obtained by the growing process described above considering alpha (a) and beta (b) cells.

3 Percolation dynamics

During the simulated neuronal growth, a synaptic connection is implemented every time a growing dendrite overlaps any portion of the other current cells. So, as the cells develop in size and shape, they tend to form more connections. A group of connected cells is henceforth understood as a *cluster*. A natural representation of such growing structures can be immediately obtained by using graphs whose nodes correspond to the neuronal cell soma and the edges correspond to the synaptic connections. While several topological and morphometrical properties of the evolving neuronal networks can be quantified, in this work attention is concentrated on the size $S(t)$ of the cluster containing the maximum number of nodes – i.e. the *dominating cluster* – found at each time instant t (i.e. the growing stage). The sizes $S(t)$ are calculated from the graphs which are constructed as the networks evolve. The critical phenomenon of percolation is identified by looking for an abrupt transition along $S(t)$, which is related to the formation of the giant cluster [7]. After this point, the growing neuronal structure is characterized by the presence of such a giant community, which dominates the subsequent connectivity dynamics.

In the following we consider simulations for the alpha and beta types of neuronal cells, i.e. the networks involve just one of these types of neurons. Three types of simulations were considered in the present work for each

[4] A branch point along the dendritic arborization corresponds to a point where the growing dendrite bifurcates.

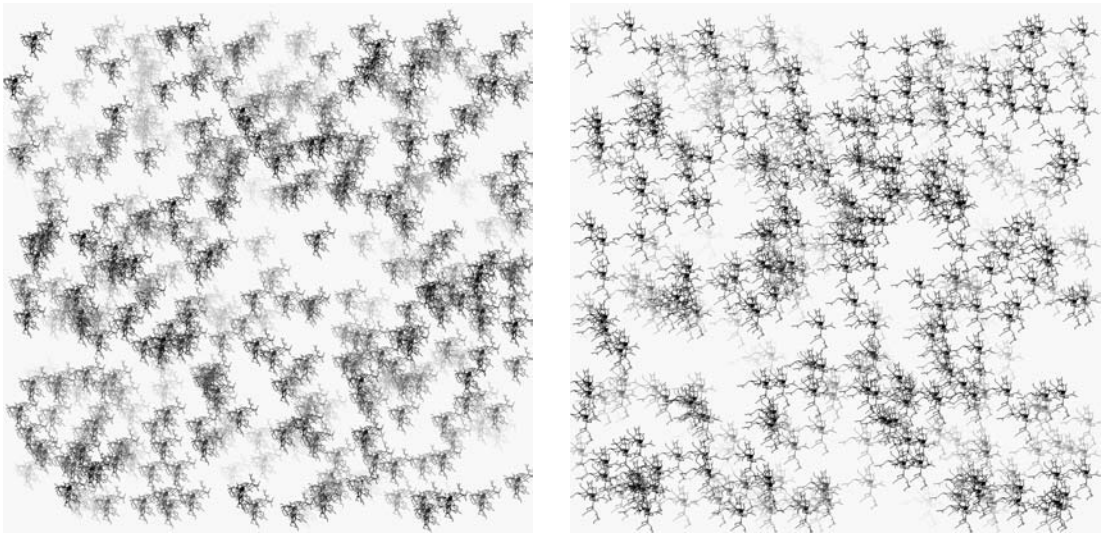

(a) (b)

Fig. 9. Examples of neuronal networks obtained by the adopted growth methodology considering the alpha (a) and beta (b) models. Different gray levels were used for neuronal cell representation in order to facilitate the visualization of the individual cells.

of the two neuronal classes: (i) just one growing neuron is considered, which is replicated in order to obtain the network, and the neuronal cells are not size-normalized; (ii) same as before, but the neurons are size-normalized; and (iii) each growing neuron is different one another (i.e. they follow the same statistical densities, but are sampled independently), and all neurons are size normalized. In all these three cases, the chosen neuronal model is "stamped" N times on the considered space (a rectangular window of 1000 by 1000 elements) according to the uniform probability. In the first and second cases, new soma positions are randomly selected at each realization, while the cell shape is kept constant. In the third case, the cell positions remain fixed at all times, but a new single cell shape is selected and used for all positions in each realization.

A total of 500 realizations was performed for each considered configuration, from which the average and standard deviation shown in the graphs were obtained. In order to avoid intense superposition between cells, cells were placed at least 5 pixels apart one another. The size normalization takes the average diameter $\langle d_{beta} \rangle$(understood as the largest distance between any two points in the cell) of the beta cells as a reference for mapping (through a scaling transformation) all the alpha cells so that their average diameter becomes equal to $\langle d_{beta} \rangle$.

Situations (i) and (ii) have been considered in order to keep statistical variability low and allow a more precise identification of the percolation critical point (not a density as in traditional percolation theory, but a time instant during the neuronal outgrowth). Situation (iii) is more realistic, but implies larger variance. The three cases, including alpha and beta realizations, are illustrated in Figures 10−12, respectively.

Figures 10a−d presents the evolution of the maximum cluster size considering growing densities of alpha cells, while Figures 10e−h presents analogous graphs considering beta cells. As expected, the critical transition tends to increase with the density of neurons, with markedly sharper transition being verified for the beta neuronal cells. Note that the percolation takes place sooner for the alpha cells because of their substantially larger sizes.

Figure 11 presents the maximum cluster size in terms of the growth stages for alpha (a−d) and beta (e−h) neurons. Unlike the previous case, the the beta cells percolate sooner than the alpha. More specifically, percolation was typically observed after 400 added beta cells, but only after 600 incorporated alpha cells. Because these two types of cells now have the same average diameter, the fact that the beta neurons now percolate sooner should be understood as a consequence of the greater "complexity" of the beta cells, in the sense of presenting a more intricated morphology. As indicated in Figure 6, which describes the cumulative two-variated distribution of dendritic segment angles, beta cells are characterized by higher dispersion of angles, implying the overall dendrites to become more disordered and spatially complex, which is in full agreement with the obtained percolation dynamics, i.e. more complex neuronal cells tend to percolate sooner than less complex cells with similar sizes.

Figure 12 presents the maximum cluster size in terms of the growth stages for alpha (a−d) and beta (e−h) neurons in the case the shapes of the size-normalized neurons in each simulation were allowed to be different. Compared to the previous case, shown in Figure 11, these simulations were characterized by a much larger dispersion of cluster size values, as indicated by the larger error bars. Interestingly, the average values obtained for the alpha (a−d) and

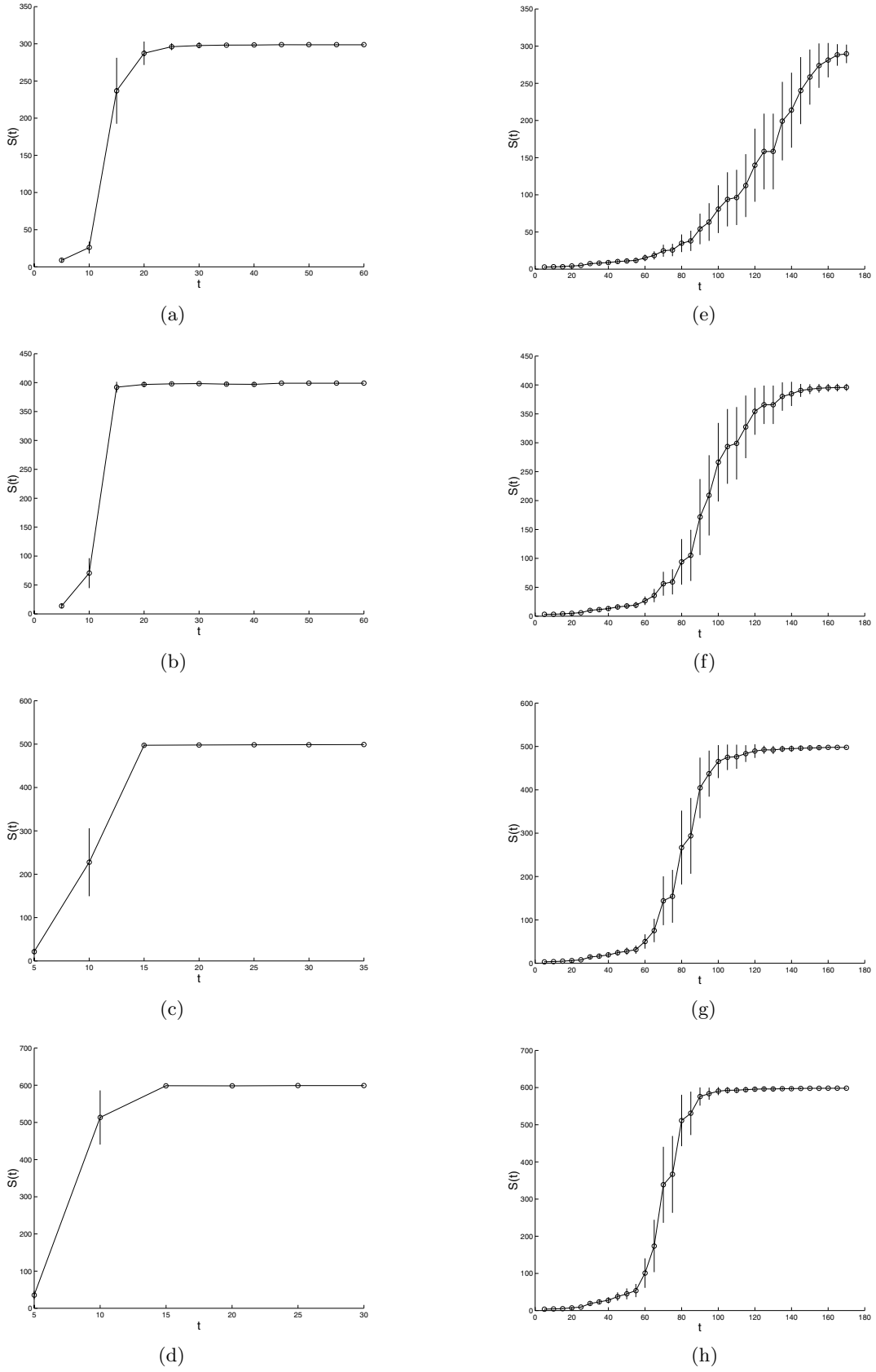

Fig. 10. Mean and standard deviation of the size of the largest cluster in terms of increasing densities (300, 400, 500 and 600 cells) of alpha and beta cells. In this case, the alpha cells are not size normalized.

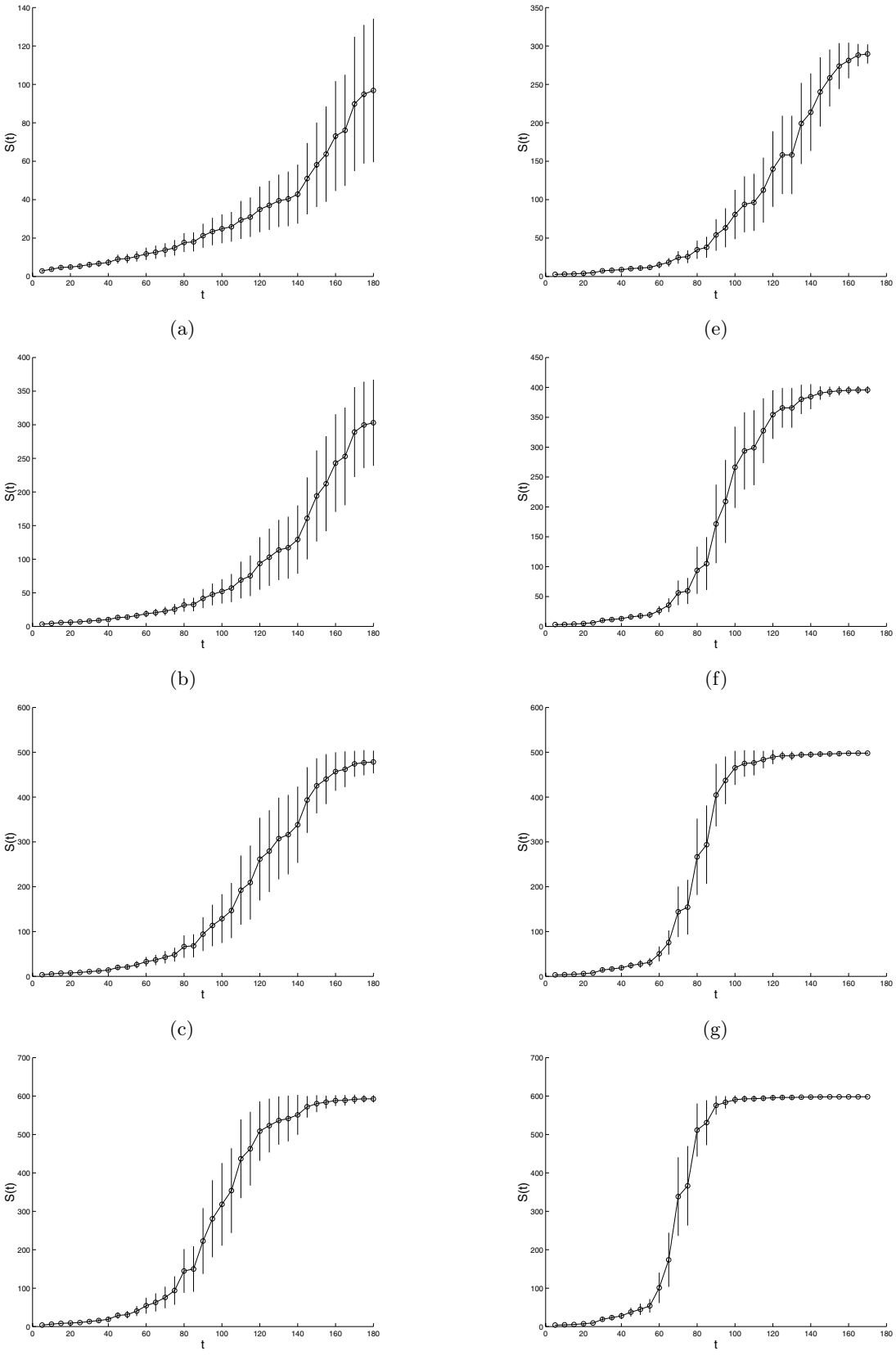

Fig. 11. Mean and standard deviation of the size of the largest cluster in terms of increasing densities (300, 400, 500 and 600 cells) or normalized alpha (a−d) and beta (e−h) cells.

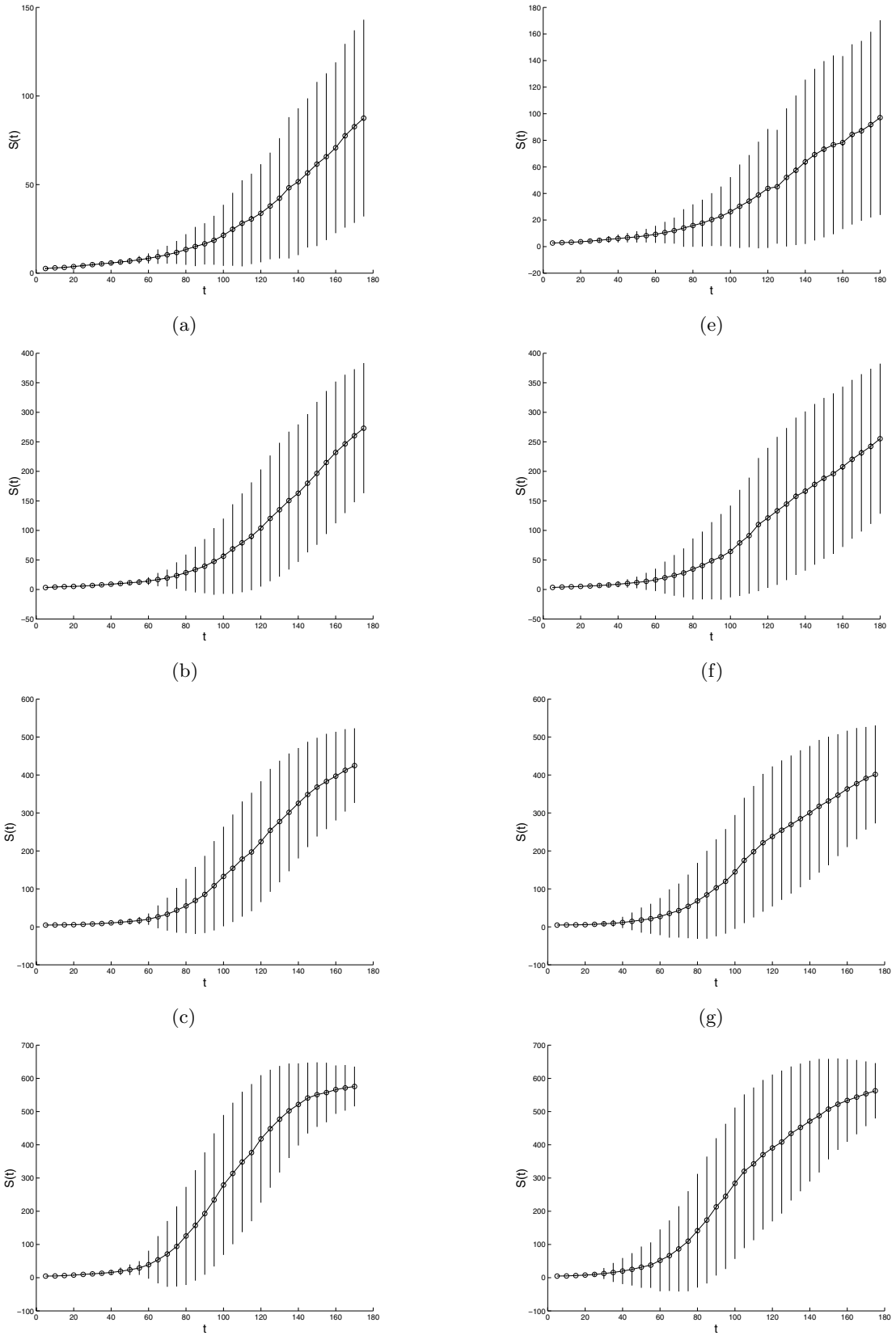

Fig. 12. Mean and standard deviation of the size of the largest cluster in terms of increasing densities (300, 400, 500 and 600 cells) of alpha (a−d) and beta (e−h) cells using the same positions of the soma and different cell morphologies drawn.

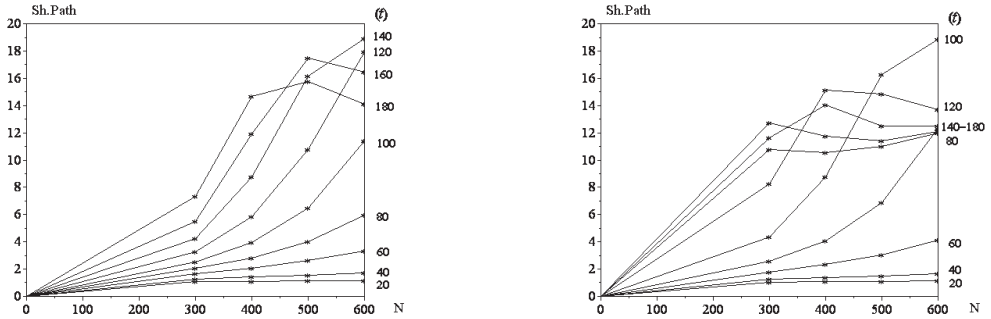

Fig. 13. The mean shortest paths in terms of the network size N obtained at several network growth stages t for alpha (a) and beta (b) cells. The neurons used in these simulations were size-normalized.

beta (e−h) cases are markedly similar, indicating that the consideration of different cell neuronal shapes from the same class tended to equalize the evolution of the overall average connectivity. Indeed, when size-normalized (which is the case), alpha and beta cells tend to present some substantial morphological similarity [20], accounting for the above observed phenomenon.

The mean shortest path between nodes, an important feature of complex networks, was also monitored during the neuronal growth for normalized size cells. Figure 13 show, with respect to alpha (a) and beta (b) cells, the shortest path in terms of the network size (i.e. the number of nodes N) at several instants t during the network evolution. The shortest path was calculated in the traditional fashion (e.g. [5]), i.e. each disconnected pair of edges was assigned the mean shortest path value among the existing pairs of nodes. Observe that different evolution of the average shortest paths have been obtained for the two different categories of neural cells, with the beta cells tending to imply overall shortest paths for $N > 300$.

4 Concluding remarks

This article has reported on several new perspectives related to neuromorphic models and percolation induced by dendritic growth. First, we have shown how morphologically realistic neuronal networks can be simulated by using Monte-Carlo sampling of statistical models derived from a series of geometrical measurements of real neuronal cells. Second, we have investigated a new perspective to percolation studies in which, instead of incorporating new connections of fixed size between the involved elements, the percolation dynamics is defined by the progressive growth of dendrites/axons, following biologically-realistic rules derived from experimental data. The obtained results indicate that the percolation in such evolving systems is also characterized by abrupt transitions of the dominating cluster size along the progression of the growth and connections. We have shown that distinct critical points are usually identified for growing dynamics of systems underlain by distinct neuronal morphologies. Three different simulation cases have been considered, involving equal and different cells and the presence or absence of size-normalization. The simulations assuming identical size-normalized cells implied that beta cells reached percolation sooner than alpha cells, a result that is related to the fact that the dendritic processes of beta cells tend to be more intrincated and spatially complex.

The mean shortest paths calculates at several growth stages were also considered. Because the mean values of such a measurement clearly do not fall in sublogarithm fashion with N, it can be safely concluded that the morphologically realistic networks obtained in the present work are not of the small-world type [5]. Actually, we have verified that the size and shape uniformity of the neurons, even when not normalized, tend to imply regularity to the networks (in the sense of uniform node degree), therefore avoiding small-world effects. Different results can be obtained by using neurons with logarithmic distribution of size, which can even lead to scale-free properties.

Such results establish and interesting connection between the statistical geometrical features of the considered cells and their potential for forming clusters among the neuronal milieu. Such perspectives and results are particularly interesting because the functional properties of neuronal networks are closely related to their connectivity (e.g. [12,14,21,22]). The perspectives for further investigations are many. For instance, it would be particularly interesting to check how the consideration of more than one distinct statistical model of neuronal geometry will affect the measured critical point. Another interesting possibility is to investigate, in the spirit of [21], to what extent the critical point statistics can be used as a resource for classification of the morphological types of involved neuronal cells. A third promising future development is to quantify, through simulations, how the geometrical properties of the neuronal cells (e.g. [22]), by controlling the sizes of the neuronal clusters, ultimately define the functional properties of the obtained structures [14]. Still, it would be interesting to correlate several measurements from complex network research, especially those related to the hierarchical structure of the networks [23], with the critical percolation time.

Luciano da F. Costa is grateful to FAPESP (processes 99/12765-2) and CNPq (process 308231/03-1) for financial support. The authors thank L.A. Consularo for tracing the neural cells and to Luis Diambra, Marconi S. Barbosa and Gonzalo Travieso for reviewing and commenting on this work.

References

1. E.R. Kandel, J.H. Schwartz, T.M. Jessel, *Essentials of neural science and behavior* (Appleton and Lange, Englewood Cliffs, 1995)
2. A. van Ooyen, Network **5**, 401 (1994)
3. A. van Ooyen, J. van Pelt, M.A. Corner, J. Theor. Biol. **172**, 63 (1995)
4. R. Albert, A.L. Barabási, Rev. Mod. Phys. **74**, 47 (2002)
5. M.E.J. Newman, SIAM Review **45**, 167 (2003), e-print `cond-mat/0303516`
6. S.N. Dorogovtsev, J.F.F. Mendes, Advances in Physics **51**, 1079 (2002), e-print `cond-mat/0106144`
7. D. Stauffer, A. Aharony, *An introduction to percolation theory*, 2nd edn. (Taylor and Francis, 1991)
8. J. Karbowski, Phys. Rev. Lett. **86**, 3674 (2003)
9. O. Shefi, I. Golding, R. Segev, E. Ben-Jacob, A. Ayali, Phys. Rev. E **66**, 021905 (2002)
10. Luciano da F. Costa, Edson Tadeu M. Monteiro, Neuroinformatics **1**, 65 (2003)
11. R. Segev, M. Benveniste, Y. Shapira, E. Ben-Jacob, Phys. Rev. Lett. **90**, 168101 (2003)
12. D. Stauffer, A. Aharony, L. da F. Costa, J. Adler, Eur. Phys. J. B **32**, 395 (2003)
13. L. da F. Costa, D. Stauffer, Physica A **330**, 37 (2003)
14. L. da F. Costa, M.S. Barbosa, V. Coupez, D. Stauffer, Brain and Mind **4**, 91 (2003)
15. G.A. Ascoli, J.L. Krichmar, Neurocomputing **48**, 1003 (2000)
16. R.C. Coelho, L. da F. Costa, Neurocomputing **48**, 555 (2001)
17. H. Waessle, H. Peichl, B.B. Boycott, Proc. Roy. Soc. London **212**, 157 (1981)
18. H. Waessle, B.B. Boycott, R.-B. Illing, Proc. Roy. Soc. London **212**, 177 (1981)
19. L. da F. Costa, R. Marcondes Cesar Jr, *Shape Analysis and Classification: Theory and Practice* (CRC Press, Boca Raton, 2001)
20. B.B. Boycott, H. Wassle, J. Physiol. **240**, 397 (1974)
21. L. da F Costa, E.T. Monteiro Manoel, F. Faucereau, J. Chelly, J. van Pelt, G. Ramakers, Network: Comput. Neural Syst. **13**, 283 (2002)
22. L. da F. Costa, T. Velte, J. Comp. Neurol. **404**, 33 (1999)
23. L. da F. Costa, Phys. Rev. Lett. **93**, 98702 (2004), e-print `cond-mat/0312646`